Eur. Phys. J. B **34**, 63–67 (2003)
DOI: 10.1140/epjb/e2003-00197-0

THE EUROPEAN PHYSICAL JOURNAL B

Electron-phonon interaction in carbon clathrate hex-C_{40}

I. Spagnolatti, M. Bernasconi[a], and G. Benedek

Dipartimento di Scienza dei Materiali and Istituto Nazionale per la Fisica della Materia,
Università degli Studi di Milano-Bicocca, Via Cozzi 53, 20125 Milano, Italy

Received 21 March 2003
Published online 23 July 2003 –

Abstract. The electron-phonon interaction in Li-doped carbon clathrates hex-LiC_{40} and hex-Li_2C_{40} has been investigated from first principles. Although the characteristic phonon frequency and electron-phonon interaction are large, the electronic density of states is relatively low which finally gives an electron-phonon coupling constant $\lambda = 0.46$ for Li_2C_{40}. Hole-doping is expected to provide higher T_c than n-doping in hex-C_{40}.

PACS. 71.15.Mb Density functional theory, local density approximation, gradient and other corrections – 74.70.Wz Fullerenes and related materials – 74.10.+v Occurrence, potential candidates

1 Introduction

The discovery of superconductivity in MgB_2 at 36 K [1] has led to a resurgence of interest in superconductivity of low-Z materials, metallic or made metallic by doping. For instance, theoretical calculations have recently suggested interesting superconductive properties in Li_xBC [2] and lithium boride [3] compounds. Purely carbon-based materials are also interesting superconductors in the form of C_{60} fullerites [4]. Both in fullerenes and in borates, superconductivity is driven by a strong electron-phonon coupling in states with large σ-character. In MgB_2 and LiBC, the conduction states are in fact purely σ-bands, while in fullerenes a partial σ-character of the conduction bands (with mainly π-character) is produced by the curvature of the cage-like structure. Smaller fullerenes (C_{36}, C_{28}, C_{20}) with a larger curvature have been predicted to have larger electron-phonon coupling [5–9] and possible solid forms of C_{36} [8] and C_{20} [9] clusters have been also proposed recently. It is suggestive to wonder what would the electron-phonon coupling be in a carbon material with conduction bands of pure σ-character, *i.e.* in a diamond-like, tetrahedral form of carbon. Metallization of diamond-like carbon by n-doping is however problematic. Although claims of diamond doping with sulfur [10] and phosporous [11] recently appeared in literature, the realization of tetrahedral carbon with high density of carriers at low temperatures suitable to display interesting T_c is far from being accomplished. In a recent paper, we have proposed an alternative form of tetrahedral carbon suitable to be heavy-doped n-type [12]. Based on *ab initio* calculations, we have shown that the tetrahedrally bonded hexagonal carbon clathrate hex-C_{40} is n-dopable by lithium insertion. The n-doping is realized by inserting the lithium atoms in the large cages of the clathrate structure. Although clathrate structures are realized experimentally for Si and Ge [13], their carbon analogs have not been synthesized so far. However, recent progress in the synthesis of carbon films by supersonic cluster beam deposition (SCBD) have shown that carbon nanostructured thin films, grown by this technique, display a variety of morphologies. For instance, evidence of the synthesis of random schwarzites has been recently provided [14]. Since, crystalline clathrates can be described as produced by the coalescence of fullerenic-like cages which is reminiscent of the growth conditions by cluster assembling in SCBD technique, one could envisage that carbon clathrate might be produced by SCBD under suitable conditions.

In this work we have studied from first-principles the electron-phonon coupling in the carbon clathrate hex-C_{40} doped with lithium, aiming at estimating its potential superconductive properties. Structural properties and electronic band structure for the pure and lithium doped phases have been studied in our previous work [12].

2 Computational details

The calculations have been performed within density functional theory in the local density approximation. Norm-conserving pseudopotential and plane wave expansion of the Kohn-Sham orbitals up to a kinetic cutoff of 40 Ry have been used, as implemented in the codes CPMD [15,16] and PWSCF and PHONONS [17]. Geometry optimization and band structure calculations have

[a] e-mail: marco.bernasconi@unimib.it

been performed by integration over a uniform grid of 36 k-points in the irreducible part of the Brillouin Zone. Calculation of phonon modes and electron-phonon coupling constant has been restricted to the Γ-point only as described below.

The strength of the electron-phonon interaction is usually expressed in terms of the electron phonon coupling constant λ as

$$\frac{\lambda}{N(0)} = \sum_{\alpha} \int \frac{\mathrm{d}\mathbf{q}}{\Omega_{\mathrm{BZ}}} \frac{\lambda_{\alpha\mathbf{q}}}{N(0)} \tag{1}$$

$$= \sum_{\alpha} \int \frac{\mathrm{d}\mathbf{q}}{\Omega_{\mathrm{BZ}}} \frac{1}{\omega^2_{\alpha\mathbf{q}}} \sum_{n,m} \int \frac{\mathrm{d}\mathbf{k}}{\Omega_{BZ}} \frac{\delta(E_{\mathbf{k}n})\delta(E_{\mathbf{k}+\mathbf{q}m})}{N^2(0)}$$

$$\times \mid \langle u_{\mathbf{k}+\mathbf{q},m} \mid \mathbf{M}^{-\frac{1}{2}} \boldsymbol{\epsilon}_{\alpha\mathbf{q}} \nabla V^{\mathbf{q}}_{\mathrm{eff}} \mid u_{\mathbf{k},n} \rangle \mid^2 \tag{2}$$

where $N(0)$ is the electronic density of states at the Fermi level (zero of energy) per spin and per cell, $\lambda_{\alpha\mathbf{q}}/N(0)$ is the partial electron-phonon coupling due the αth phonon at the point $\mathbf{q}$ in the BZ (of volume Ω_{BZ}), $\boldsymbol{\epsilon}_{\alpha\mathbf{q}}$ is the phonon polarization vector, $\mathbf{M}$ is the atomic mass matrix, n and m are electronic band indices, $u_{\mathbf{k},n}$ is the periodic part of the Kohn-Sham state with energy $E_{\mathbf{k}n}$, and $\nabla V^{\mathbf{q}}_{\mathrm{eff}}$ is the derivative of the Kohn-Sham effective potential with respect to the atomic displacement caused by a phonon with wavevector $\mathbf{q}$. The evaluation of equation (2) requires a double integral over the BZ which is computationally very demanding for hex-C_{40}. However, for systems with low dispersion of the phononic and electronic bands (around the Fermi energy), a reliable estimate of $\lambda/N(0)$ can be obtained in the so-called molecular-like approximation as [20,21]

$$\frac{\lambda}{N(0)} = \sum_{\alpha} \frac{1}{\omega^2_{\alpha} g^2} \sum_{n,m}^{g} \mid \langle u_m \mid \mathbf{M}^{-\frac{1}{2}} \boldsymbol{\epsilon}_{\alpha} \nabla V_{\mathrm{eff}} \mid u_n \rangle \mid^2 \tag{3}$$

where the sum over α and n, m run over the phonons and the g degenerate electronic states at the Fermi level at the Γ point, respectively. As to the applicability of equation (3) to systems like hex-C_{40}, we note that the bandwidth of LiC_{40} and Li_2C_{40} (*cf.* Fig. 2) from the bottom of the conduction band to E_F is comparable to that of a C_{20}-based solid for which the molecular-like approximation has been demonstrated to be highly accurate [9].

3 Results

The clathrate hex-C_{40}, proposed theoretically in references [12,18] is shown in Figure 1. It belongs to the space group P6/mmm and has 40 atoms per unit cell, the symmetry independent atoms being five. The structure can be seen as resulting from the coalescence (by sharing hexagonal and pentagonal rings) of two C_{26}, two C_{24} and three C_{20} cages per unit cell, which gives rise to a hexagonal array of parallel tubes, each tube being an infinite pile of C_{24} cages. The tubes in turn are held together by rings of C_{26} and C_{20} cages arranged on alternate planes normal to the tubes. As discussed in our previous work [12], Li can be inserted at the center of the C_{26} and C_{24} cages with small changes in the equilibrium cell parameters (within 1%). At low Li content (LiC_{40}), the band structure does not change significantly with respect to the pure compound, but for the shift of the Fermi level inside the conduction bands and a small downward shift in energy of the lowest conduction band at the Γ point. Therefore, the

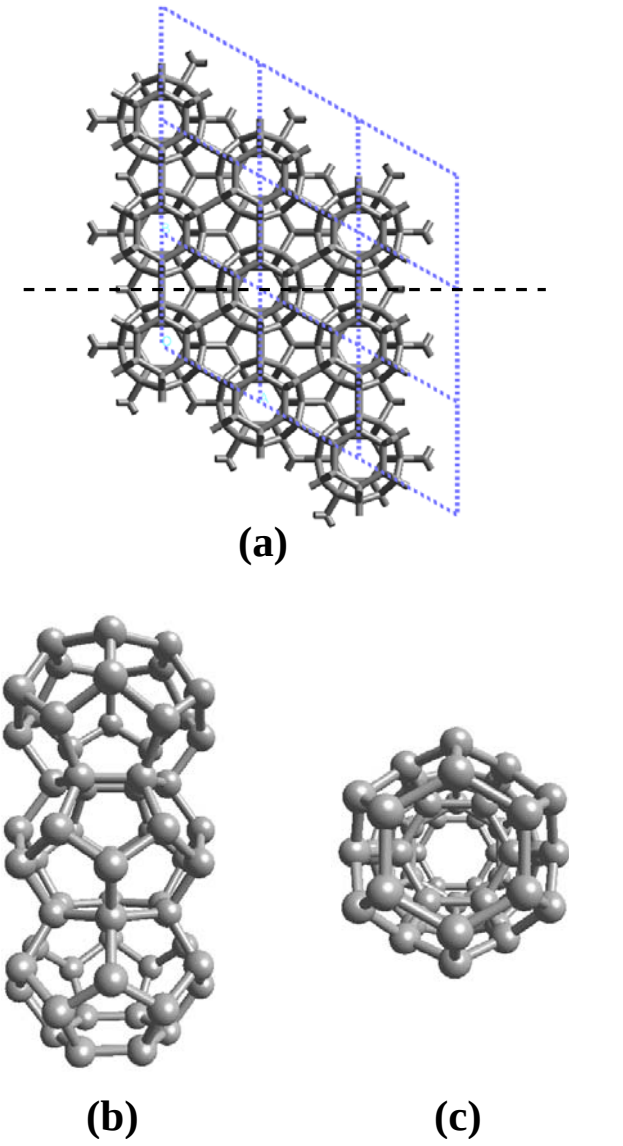

Fig. 1. Structure of the clathrate hex-C_{40}. (a) View of the plane perpendicular to the c axis. Chains of C_{24} cages form channels running along the c direction, arranged in a hexagonal array in the plane. (b) Side view of one channel. (c) Top view of one channel. The position of the five symmetry-independent atoms in crystal coordinates are: (−0.667, −0.333, 0.112), (−0.247, −0.247, 0.500), (−0.379, −0.379, 0.309), (−0.211, −0.421, 0.186), (−0.132, −0.263, 0.000) [12]. In Li_2C_{40} the Li ions in the C_{26} cages are at positions: (0.333, 0.667, 0.500), (0.667, 0.333, 0.500).

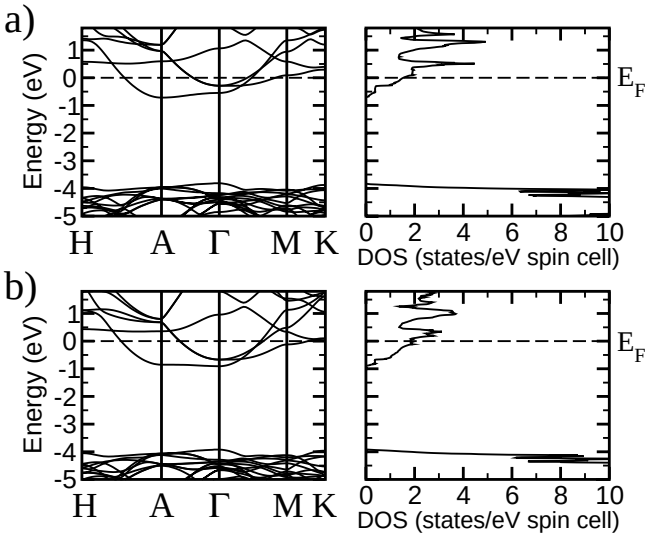

Fig. 2. Electronic energy bands around the Fermi level (E_F) of a) LiC_{40} and b) Li_2C_{40}. The Li ions are at the centre of the C_{26} cages. The band structure is reported along the high symmetry lines of the irreducible Brillouin Zone following the notation of reference [19]. Density of states are computed by the tetrahedron method over a mesh of 270 points in the irreducible BZ.

electronic properties of the system at low Li content can be described in the rigid-band approximation where Li is fully ionized and donates its outermost electron to the host without changing the band structure (Fig. 2a). At higher Li concentration (Li_2C_{40}) deviations from the rigid-band approximation are appreciable (Fig. 2b).

We have thus applied equation (3) to compute the electron-phonon coupling in hex-C_{40}. Since the rigid band approximation holds to a large extent in Li_xC_{40} we have computed the electron-phonon coupling $\lambda/N(0)$ given by equation (3) for the pure system with an additional electron in the lowest conduction band, mimicking LiC_{40}. At the Γ-point the lowest conduction band is non-degenerate and thus only a single electronic state and phonons with A_{1g} character contribute to the sum in equation (3). The shape of the Kohn-Sham orbital of the lowest conduction at the Γ-point which contributes to $\lambda/N(0)$ is shown in Figure 3 for Li_2C_{40}. The charge density of this state is mostly localized in the C_{26} cages and it is polarized by the Li ions.

Phonon frequencies and eigenvectors have been obtained by diagonalization of the dynamical matrix at the Γ-point, built from the numerical derivatives of the forces with respect to finite atomic displacements. The change in the effective potential due to the αth phonon is computed by finite differences as

$$\boldsymbol{\epsilon}_\alpha \cdot \nabla V_{\text{eff}} = (V_{\text{eff}}(\mathbf{r} + h\boldsymbol{\epsilon}_\alpha) - V_{\text{eff}}(\mathbf{r} - h\boldsymbol{\epsilon}_\alpha))/2h, \qquad (4)$$

where $\mathbf{r}$ indicate collectively the equilibrium atomic positions. Integration of the BZ in the calculation of ∇V_{eff} in equation (4) has been restricted at the Γ-point as well.

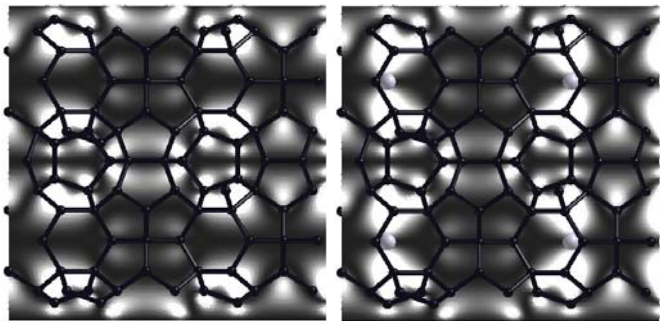

Fig. 3. Density plot of the KS state at the Γ point of the lowest conduction band for pure C_{40} (left panel) and Li_2C_{40} (right panel). The plane of the figure is the $(2\bar{1}\bar{1})$ plane passing through the center of the C_{26} cages. Light regions correspond to higher electron density. The KS state is mostly localized on the carbon atoms of the C_{26} cages and it is strongly polarized by the Li ions at the center of the cages. Small dark and large light gray spheres denote carbon and Li atoms, respectively.

Table 1. Partial electron-phonon coupling constant $\lambda_\alpha/N(0)$ in hex-C_{40}, doped with an additional electron. The energies of the modes for the undoped hex-C_{40} are reported.

Modes	Undoped	$\lambda_\alpha/N(0)$
	Energy (cm^{-1})	(eV)
$A_{1g}(7)$	1284	0.027
$A_{1g}(6)$	1212	0.040
$A_{1g}(5)$	1144	0.148
$A_{1g}(4)$	1019	0.029
$A_{1g}(3)$	932	0.000
$A_{1g}(2)$	799	0.004
$A_{1g}(1)$	649	0.000
$\sum A_{1g}$		0.248

Frequency and partial electron-phonon coupling constants for each A_{1g} normal mode are reported in Table 1. The mode $A_{1g}(5)$ that gives the largest contribution to $\lambda/N(0)$ is shown in Figure 4. The total electron-phonon coupling constant is $\lambda/N(0) = 0.248$ eV which is substantially larger than theoretical estimates for C_{60} (0.07 eV [9,21]). In order to estimate the error in $\lambda/N(0)$ due the rigid band approximation, we have computed the energy shift of the lowest conduction state at Γ in Li_2C_{40} (*cf.* Fig. 2), induced by the $A_{1g}(5)$ frozen phonon. It turns out that the rigid band approximation introduces an error in $\lambda/N(0)$ lower than 9% for the Li_2C_{40} compound. By careful BZ integrations we have checked that an additional error of 10% is possibly due to the use of the Γ-point only in the calculation of ∇V_{eff} in equation (3). Thus, an overall error of up to 20% in the value of $\lambda/N(0)$ is possible. Still, within

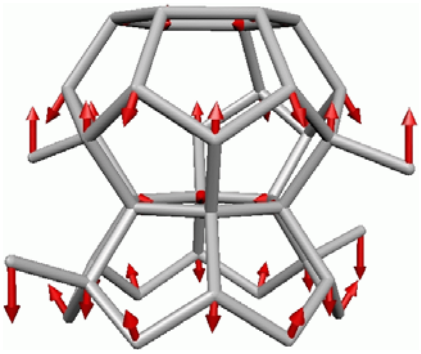

Fig. 4. Displacement pattern of the mode at 1144 cm^{-1} that gives the largest contribution to the electron-phonon coupling.

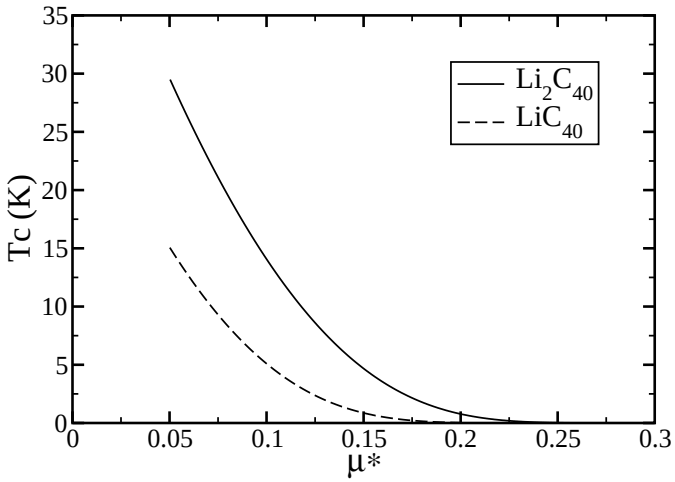

Fig. 5. Superconducting critical temperature of Li_2C_{40} and Li_1C_{40} as a function of μ^* obtained from the McMillan formula and using the values for λ and ω_{ln} reported in the text.

these uncertainties, we can try to estimate T_c by making use of the McMillan's solution [22,23] of the Eliashberg equations:

$$T_c = \frac{\omega_{ln}}{1.2}\exp\left(-\frac{1.04(1+\lambda)}{\lambda-\mu^*(1+0.62\lambda)}\right), \qquad (5)$$

where ω_{ln} is the weighted logarithmic average of the phonon frequencies (1145 cm^{-1} for hex-C_{40}) and μ^* is the renormalized Coulomb pseudopotential [22,23]. From the density of states (DOS) in Figure 2, we obtain $N(0) = 1.55$ or 1.85 states/eV/spin/cell and thus $\lambda = 0.38$ and 0.46, for LiC_{40} and Li_2C_{40}, respectively. We have not attempted to estimate numerically μ^*. Instead the resulting T_c is plotted in Figure 5 as a function of μ^* in the range typical of simple and transition metals. Although the characteristic phonon frequency and the electron-phonon interaction potential $\lambda/N(0)$ are comparable or even larger than in other low-Z superconductors (MgB_2, C_{60}), the electronic DOS at the Fermi level is low in Li_2C_{40} and the resulting low value of λ makes the estimate of T_c strongly dependent on the choice of μ^*, even in the relatively narrow range of $\mu* = 0.1-0.15$. A reliable estimate of T_c is thus possible only for its upper bound. However, we note that the electronic DOS is much larger for the top valence bands than for the lowest conduction bands (*cf.* Fig. 2). Moreover, the electron-phonon coupling constant $\lambda/N(0)$ for the valence band, obtained by inserting in equation (3) the uppermost KS state at Γ is $\lambda/N(0) = 0.33$ eV, even larger than for the conduction bands. Hole-doping seems more promising than n-doping to make hex-C_{40} superconducting at high temperatures.

4 Conclusions

Based on density functional theory, we have computed the electron-phonon coupling constant of the carbon clathrate hex-C_{40} doped with Li at different concentrations, LiC_{40} and Li_2C_{40}. These systems, proposed on a solely theoretical basis have not been synthesized so far, but they are interesting as example of a metallic phase of tetrahedral carbon. Characteristic phonon frequencies and electron-phonon interaction potential ($\lambda/N(0)$) are large in these systems, but the low concentration of conduction electrons and the conduction bandwidth, as produced by the tetrahedral network, make the electronic DOS at the Fermi level relatively low which finally yields $\lambda = 0.38-0.46$ for LiC_{40} and Li_2C_{40}, respectively. For λ in this range, the estimate of T_c from McMillan equation is strongly dependent on the value chosen for the coulomb pseudopotential parameter μ^*. However, the calculation predicts a much larger DOS and comparable $\lambda/N(0)$ for hole-doped hex-C_{40}. Insertion of electron acceptor species in the clathrate cages seems a more promising route to make hex-C_{40} superconducting.

This work is partially supported by the INFM Parallel Computing Initiative, and by MURST, through PRIN01 under contract 2001021133.

References

1. J. Nagamatsu *et al.*, Nature **410**, 63 (2001)
2. H. Rosner *et al.*, Phys. Rev. Lett. **88**, 127001 (2002)
3. S. Gunji, H. Kamimura, Phys. Rev. B **54**, 13665 (1996)
4. A.F. Hebard *et al.*, Nature **350**, 600 (1991)
5. A. Devos, M. Lannoo, Phys. Rev. B **58**, 8236 (1998)
6. N. Breda, R.A. Broglia, G. Colò, G. Onida, D. Provasi, E. Vigezzi, Phys. Rev. B **62**, 130 (2000)
7. G.B. Adams, O.F. Sankey, J.B. Page, M. O'Keeffe, Chem. Phys. **176**, 61 (1993)
8. J.C. Grossman, S.G. Louie, M.L. Cohen, Phys. Rev. B **60**, R6941 (1999)
9. I. Spagnolatti, M. Bernasconi, G. Benedek, Europhys. Lett. **59**, 572 (2002)
10. I. Sakaguchi *et al.*, Phys. Rev. B **60**, 2139 (1999)

11. N. Fujimori *et al.*, Mat. Res. Soc. Symp. Proc. **162**, 23 (1990); A.E. Alexenko, B.V. Spitsyn, Diamond Relat. Mater. **1**, 705 (1992); S. Koizumi *et al.*, Appl. Phys. Lett. **71**, 1065 (1997); T. Saito *et al.*, Jpn J. Appl. Phys., Part 2 **37**, L543 (1998); N. Nesládek *et al.*, Phys. Rev. B **59**, 14852 (1999)
12. M. Bernasconi, S. Gaito, G. Benedek, Phys. Rev. B **61**, 12689 (2000)
13. J.S. Kasper *et al.*, Science **150**, 1713 (1965)
14. P. Milani *et al.*, J. Appl. Phys. **82**, 5793 (1997); P. Milani, S. Iannotta, *Cluster Beam Synthesis of Nanostructured Materials*, Springer Series in Cluster Physics (Springer-Verlag, Berlin, 1999)
15. CPMD version 3.0, developed by J. Hutter *et al.*, Max-Planck-Institut für Festkörperforschung and IBM Research Laboratory (1990–2001)
16. D. Marx, J. Hutter, in *Modern Methods and Algorithms of Quantum Chemistry*, edited by J. Grotendorst (John von Neumann Institute for Computing, Jülich, NIC Series, Vol. 1, 2000), pp. 301–449
17. PWSCF and PHONON codes developed by S. Baroni, P. Giannozzi, S. de Gironcoli, A. Dal Corso and others, Sissa, Trieste, `http://www.pwscf.org`
18. G. Benedek *et al.*, Chem. Phys. Lett. **244**, 339 (1995); G. Benedek and L. Colombo, in *Cluster Assembled Materials*, edited by K. Sattler (Trans. Tech. Publ. Winthertur, 1997), p. 1; G. Benedek *et al.*, in *Proceeding of the International School of Physics "Enrico Fermi", Course CXXXV*, edited by A. Paoletti, A. Tucciardone (IOS PRESS, Amsterdam 1997), p. 575
19. J. Zak, *Irreducible Representation of the Space Groups* (Benjamin, New York, 1969)
20. M. Schluter, M. Lannoo, M. Needels, G.A. Baraff, D. Tománek, Phys. Rev. Lett. **68**, 526 (1992)
21. O. Gunnarsson, Rev. Mod. Phys. **69**, 575 (1997)
22. J.P. Carbotte, Rev. Mod. Phys. **62**, 1027 (1990)
23. P.B. Allen, B. Mitrović, Solid State Phys. **37**, 1 (1982)